physica status solidi
pss
www.pss-journals.com

reprint

WILEY-VCH

EarlyView publication on wileyonlinelibrary.com
(issue and page numbers not yet assigned;
citable using Digital Object Identifier – **DOI**)

Phys. Status Solidi B, 1–4 (2012) / **DOI** 10.1002/pssb.201200446

physica status solidi b
www.pss-b.com
basic solid state physics

On the low temperature microwave absorption anomaly in single-wall carbon nanotubes

Anita Karsa[1], Dario Quintavalle[1], László Forró[2], and Ferenc Simon[*,1]

[1] Budapest University of Technology and Economics, Institute of Physics and Condensed Matter Research Group of the Hungarian Academy of Sciences, 1521 Budapest, Hungary
[2] Institute of Physics of Complex Matter, FBS Swiss Federal Institute of Technology (EPFL), 1015 Lausanne, Switzerland

Received 3 July 2012, accepted 18 September 2012
Published online 12 November 2012

Keywords carbon nanotubes, graphene, microwave conductivity

[*] Corresponding author: e-mail ferenc.simon@univie.ac.at, Phone: +36 1 4633816, Fax: +36 1 4634180

The low temperature microwave absorption anomaly reported by Corzilius et al. [Phys. Rev. B **75**, 235416 (2007)] in single-wall carbon nanotubes (SWCNTs) is revisited. It was originally reported that the microwave absorption of CVD grown SWCNTs shows an unexpected increase below ~20 K (using flow cryostats) which depends on the microwave power. The original observation was made using the microwave cavity perturbation method while sweeping the microwave frequency. We reproduced this effect on arc-discharge based SWCNTs, using static cryogenic conditions with cooled microwave cavities, and employing a stable frequency source locked to the cavity resonance. Our observation shows that the microwave absorption anomaly is robust against the tube type and the experimental conditions.

© 2012 WILEY-VCH Verlag GmbH & Co. KGaA, Weinheim

1 Introduction Understanding the conductivity in single-wall carbon nanotubes is one of the most intensively studied subject of their research. The interest is driven by the potential applications of SWCNTs as metallic interconnects [1] or as transistor elements [2]. Early on after their discovery [3, 4] it became clear that SWCNTs are quasi one-dimensional conductors [5] whose electronic properties depend strongly on their geometry. It turned out that SWCNTs can be either metallic or semiconducting in a 1:2 ratio of abundance of these respective species [6]. This possibility of occuring as either metallic or semiconducting (insulating) would potentially endow them with an enormous application potential.

It is now clarified that metallic SWCNTs with diameters below ≈2 nm tend to form the so-called Tomonaga–Luttinger liquid [7, 8] phase [9–15] while the semiconducting SWCNTs have a diameter dependent gap of about 0.5–2 eV which is appropriate for transistor applications. In addition to their underlying tubular structure (which we shall call as "primary" structure), SWCNTs form a further hexagonal arrangement, known as bundles (as a "secondary" structure), due to the van der Waals force [16]. In a macroscopic sample, the bundles form a tertiary structure which is better known as an SWCNT "spaghetti." As a result, for a macroscopic sample the conduction is mainly limited by the bundle–bundle interaction in the tertiary structure even when in the underlying metallic SWCNTs would provide a percolating metallic network.

Kaiser et al. showed that resistivity for a macroscopic SWCNT sample is characterized by a semiconductor-like temperature dependence:

$$\varrho \propto \mathrm{e}^{T_c/T} \tag{1}$$

with a small $T_c = 10$–100 K (we use the original notation from Ref. [17]). This is due to the bundle–bundle contacts which act as finite barriers for the transport. Microwave conductivity, based on the so-called microwave cavity perturbation [18, 19], is a contactless method with relatively large sensitivity to relative changes in the conductivity but much more limited to yield the absolute value of conductivity in materials. As a result, it proved to be efficient for the characterization of air sensitive fulleride conductors [20, 21], where the conventional contacted methods proved impractical. The method relies on the measurement of the quality factor, Q, change of a

© 2012 WILEY-VCH Verlag GmbH & Co. KGaA, Weinheim

microwave cavity when the sample is placed inside. For the powder samples such as fullerides or SWCNTs, most information is gained when the sample is placed into the maximum of the microwave magnetic field and the node of the electric one. Then, it turns out that $Q \propto \varrho$, which allows a measurement of the latter quantity. The microwave conductivity essentially measures the DC value since the employed microwave frequency ($\approx$10 GHz) is much lower than a typical plasma frequency value (a few 100 THz).

SWCNTs are thought to be efficient microwave absorbing materials (which may find applications in the defense industry) due to their porous nature, large thermal stability, and good heat conductivity. However, understanding of the fundamental microwave absorption properties is necessary before the successful applications. Corzilius et al. [22, 23] presented a microwave conductivity measurement on SWCNTs using the microwave cavity perturbation method. In general, they observed a semiconducting-like temperature dependence of ϱ, that is, the temperature dependent Q was monotonically increasing with decreasing temperature. A surprising, low temperature anomaly, which was dependent on the applied microwave power, was also observed: for larger microwave powers the cavity quality factor had a maximum followed by a decreasing Q on further lowering the temperature. It was argued in the original work that the anomaly originates from a true electronic effect, which may be caused by the occurrence of superconductivity in the samples.

Motivated by this yet unexplained but intriguing phenomenon, we revisit this problem herein with several modifications in order to test its robustness against the experimental and sample conditions. We use (i) arc-discharge grown sample instead of the "super-growth" CVD samples in the previous work, (ii) using a static cryostat rather than a flow-through one in the previous work, and finally (iii) an automatic frequency control based method [24], which provides a well defined microwave irradiation condition and also a large precision measurement of the Q. We reproduce the effect seen by Corzilius et al. which shows that it is ubiquitous to the SWCNTs irrespective of the sample type and experimental conditions.

2 Experimental A TE011 microwave cavity operating with a resonance frequency of $\approx$11.2 GHz was constructed of copper and is shown in Fig. 1. Microwaves are generated by a HP83751B synthesized sweeper oscillator and were detected with a HP8473D zero bias microwave power detector. Care was taken to operate the detector with the same power level which is attained using an attenuator immediately before it. Two semi-rigid copper coaxial cables provide a transmission configuration. Both cables are terminated by inductive antennae which couple the coaxial microwave modes to the free-space modes inside the cavity. The coupling is controlled by the insertion of the antennae inside the cavity and also by rotating the plane of the induction with respect to the radial direction of the cavity. Both couplings are about 20% (i.e., only a fifth of the incoming microwaves enters the cavity). The cavity undercoupling increases the accuracy for small changes in the cavity Q factor due to the sample.

The Q measurement was essentially the method developed by Nebendahl et al. [24]. In brief, the microwave frequency is continuously modulated with a radio-frequency (e.g., 25 kHz) with a modulation magnitude comparable to the width of the cavity resonance. The detector signal is connected to two lock-in amplifiers which detect the 1st and 2nd/4th harmonics of the *rf* modulation frequency. The magnitude of the 1st harmonic is used as a feedback to keep the center of the microwave frequency on the cavity resonance. This is known as the automatic frequency control

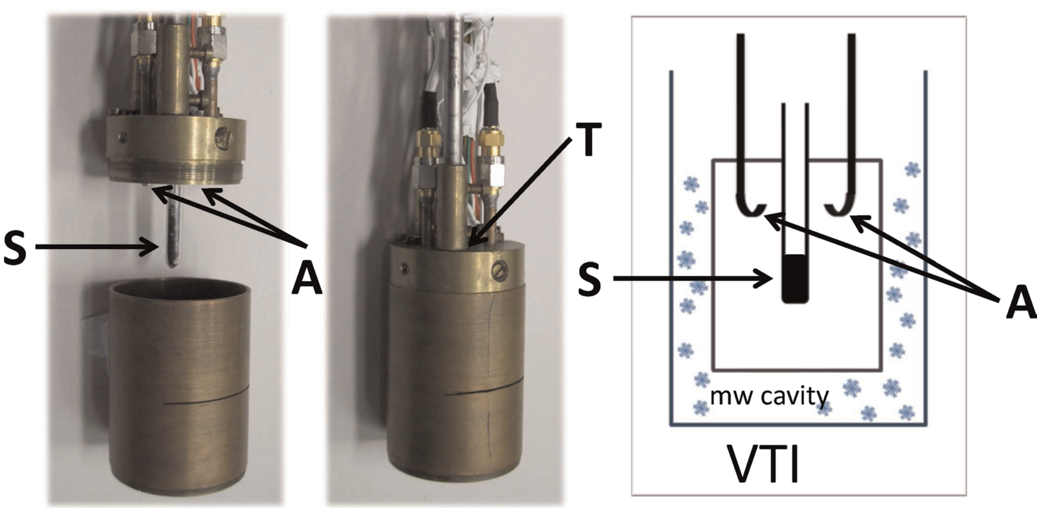

Figure 1 (online color at: www.pss-b.com) Photograph of the disassembled (left) and assembled (middle) microwave cavity probehead and its schematics (right). Arrows show the main elements; S, sample; A's, coupling antennae; T, location of the thermometer. Note the horizontal slit which suppresses the TM111 mode which is degenerate with the working mode of TE011. The sample is inside a quartz tube and is sealed under 20 mbar helium. It is located in the center of the cavity at the maximum of the microwave magnetic and in the node of the electric field.

© 2012 WILEY-VCH Verlag GmbH & Co. KGaA, Weinheim

(AFC) method [25]. It was shown in Ref. [24] that the ratio of the 2nd and 4th harmonics are a measure of the cavity resonance width without instrument dependent parameters and thus yield the Q factor directly.

The advantage of this method over the usual frequency swept method, which was used in Ref. [22], is twofold: first its noise for the measured Q is about a factor 10 better, second it provides a continuous microwave irradiation of the sample and cavity and thus avoids transient effects.

The probehead shown in Fig. 1 was embedded in a closed sample compartment which contains a constant pressure He exchange gas (typically 10 mbar) and is in thermal contact with the variable temperature insert of a 9 T superconducting magnet (Oxford Instruments). Temperature was regulated to 0.05 K accuracy with a Lakeshore 331 temperature controller and a CX-1050 thermometer. The thermometer is embedded in brass block and is placed as close as possible to the sample.

The sample was arc-discharge grown with mean diameter of 1.4 nm (Nanocarblab, Russia, Moscow) and was from a batch which was used for previous studies and has been thoroughly characterized by a number of methods [26–28]. A fine powder of the sample was placed in a quartz tube, first heated to 500 °C to remove contaminations and then sealed under 20 mbar helium exchange gas.

3 Results and discussion In Fig. 2, we show the sample quality factor, Q_s as obtained using

$$\frac{1}{Q_m} = \frac{1}{Q_0} + \frac{1}{Q_s}, \tag{2}$$

where Q_m and Q_0 are the quality factors of the measured and the unloaded cavity, respectively. Q_0 has a weak

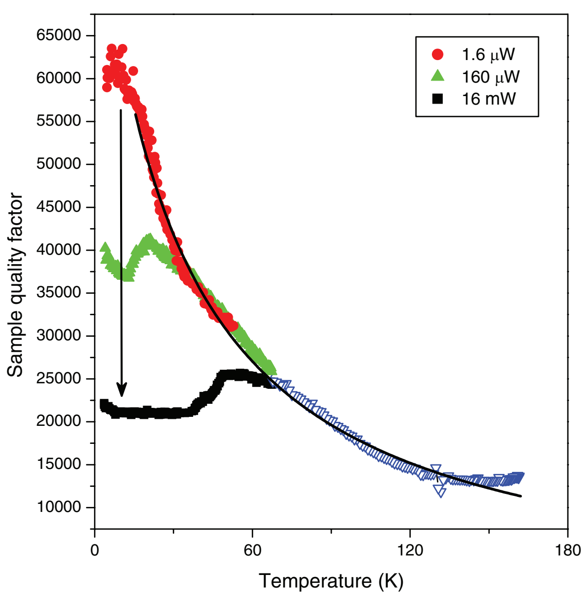

Figure 2 (online color at: www.pss-b.com) The sample quality factor obtained from Eq. (2) for different values of the incident microwave power on the cavity. The solid curve is an exponential fit to the resistivity using Eq. (1) with $T_c = 45$ K.

temperature dependence and it was obtained in a reference measurement without the sample. Figure 2 shows the Q_s data for different values of the microwave power incident on the cavity, which also takes into account the undercoupling of the cavity and losses in the coaxial cables. There is a clear dependence of the data on the employed microwave power. The lowest incident power on the sample is 1.6 μW and we could not perform meaningful measurements of Q for even lower powers.

The Q_s data for the lowest power shows an exponential temperature dependence in the 20–150 K temperature range. This temperature dependence indicates that Q_s is indeed proportional to the resistivity which is expected for the present measurement geometry and sample morphology. Then, $Q_s \propto \varrho$ is used to extract the transport barrier height of $T_c = 45$ K according to Eq. (1). This value compares well with $T_c = 65$ K found in Ref. [17].

Below about 20 K, the Q_s data show a slight downturn for the 1.6 μW data, which is even more pronounced at higher microwave powers. This observation is in agreement with the previous observation of Corzilius et al. We underline that the effect is not related to the detection system as the power incident on the detector is constant for all values of the employed power.

For higher microwave powers, the Q_s data show a downturn whose temperature onset is higher for higher power. However, all data curves merge together around 60 K. Interestingly, even the merging of the curves is qualitatively identical to that observed in Ref. [22] as therein the merging was observed around 40–50 K except for the highest power (190 mW) where a clear heating effect was observable.

We find it surprising that the nonlinear power dependent microwave absorption (NLMWA), which was reported in Ref. [22] is reproduced for a very different nanotube sample, even when the experimental conditions in terms of cryostat type, microwave resonator, and detection technique are different. The most important difference in the sample type stems from the growth conditions: the "super-growth" CVD is known to result in SWCNTs with diameters of 2–3 nm [29] which are well isolated from one-another [30] and which are catalyst free. In contrast, the arc-discharge grown SWCNTs have a much narrower diameter distribution of 1.4 ± 0.1 nm with always a sizeable (up to 10 wt%) residual catalyst content. This suggest that the effect is related to the SWCNTs and the residual catalyst content does not play a role.

The diameter independence of the effect excludes that it is related to a phase transition due to correlation effects. It has been calculated for SWCNTs that the electron–phonon coupling (which would lead to superconductivity) is strongly nanotube diameter dependent [31, 32]. Similarly, interactions which involve electron–electron coupling are also strongly diameter dependent as the Coulomb interaction depends on the electron confinement. The observations rather suggest that the unique SWCNT structure, which contains an interlinked network of metallic wires, separated by small barriers, gives rise to this effect. A bolometric effect

© 2012 WILEY-VCH Verlag GmbH & Co. KGaA, Weinheim

as its possible origin cannot be excluded either but further work is required to settle this issue.

4 Summary In summary, we reproduced the low temperature microwave absorption anomaly in SWCNTs which was observed previously in Ref. [22]. We used different sample morphology and differing experimental methods. The result indicates that the absorption anomaly is a generic feature of SWCNTs, however its origin remains unclear.

Acknowledgements Work supported by the ERC Grant No. ERC-259374-Sylo, and by the New Szechenyi Plan No. TAMOP-4.2.2.B-10/1-2010-0009. The Swiss NSF is acknowledged for support.

References

[1] S. J. Tans, M. H. Devoret, H. Dai, A. Thess, R. E. Smalley, L. J. Geerligs, and C. Dekker, Nature **386**, 474–477 (1997).
[2] A. Bachtold, P. Hadley, T. Nakanishi, and C. Dekker, Science **294**, 1317–1320 (2001).
[3] S. Iijima and T. Ichihashi, Nature **363**, 603–605 (1993).
[4] D. S. Bethune, C. H. Kiang, M. S. DeVries, G. Gorman, R. Savoy, and R. Beyers, Nature **363**, 605 (1993).
[5] N. Hamada, S. Sawada, and A. Oshiyama, Phys. Rev. Lett. **68**, 1579–1581 (1992).
[6] R. Saito, G. Dresselhaus, and M. Dresselhaus, Physical Properties of Carbon Nanotubes (Imperial College Press, London, 1998).
[7] S. Tomonaga, Prog. Theor. Phys. **5**, 349 (1950).
[8] J. M. Luttinger, J. Math. Phys. **4**, 1154 (1963).
[9] R. Egger and A. O. Gogolin, Phys. Rev. Lett. **79**, 5082–5085 (1997).
[10] C. Kane, L. Balents, and M. P. A. Fisher, Phys. Rev. Lett. **79**, 5086–5089 (1997).
[11] M. Bockrath, D. H. Cobden, J. Lu, A. G. Rinzler, R. E. Smalley, L. Balents, and P. L. McEuen, Nature **397**, 598–601 (1999).
[12] H. Ishii, H. Kataura, H. Shiozawa, H. Yoshioka, H. Otsubo, Y. Takayama, T. Miyahara, S. Suzuki, Y. Achiba, M. Nakatake, T. Narimura, M. Higashiguchi, K. Shimada, H. Namatame, and M. Taniguchi, Nature **426**, 540–544 (2003).
[13] B. Gao, A. Komnik, R. Egger, D. C. Glattli, and C. Bachtold, Phys. Rev. Lett. **92**, 216804-1–216804-4 (2004).
[14] H. Rauf, T. Pichler, M. Knupfer, J. Fink, and H. Kataura, Phys. Rev. Lett. **93**, 096805 (2004).
[15] Y. Ihara, P. Wzietek, H. Alloul, M. H. Rümmeli, T. Pichler, and F. Simon, Eur. Phys. Lett. **90**, 17004 (2010).
[16] A. Thess, R. Lee, P. Nikolaev, H. Dai, P. Petit, J. Robert, C. Xu, Y. H. Lee, S. G. Kim, A. G. Rinzler, D. T. Colbert, G. E. Scuseria, D. Tománek, J. E. Fischer, and R. E. Smalley, Science **273**, 483–487 (1996).
[17] A. B. Kaiser, G. Düsberg, and S. Roth, Phys. Rev. B **57**, 1418–1421 (1998).
[18] O. Klein, S. Donovan, M. Dressel, and G. Gruner, Int. J. Infrared Millim. Waves **14**(12), 2423–2457 (1993).
[19] S. Donovan, O. Klein, M. Dressel, K. Holczer, and G. Gruner, Int. J. Infrared Millim. Waves **14**(12), 2459–2487 (1993).
[20] F. Bommeli, L. Degiorgi, P. Wachter, O. Legeza, A. Jánossy, G. Oszlanyi, O. Chauvet, and L. Forro, Phys. Rev. B **51**, 14794–14797 (1995).
[21] H. Kitano, R. Matsuo, K. Miwa, A. Maeda, T. Takenobu, Y. Iwasa, and T. Mitani, Phys. Rev. Lett. **88**, 096401 (2002).
[22] B. Corzilius, K. P. Dinse, J. van Slageren, and K. Hata, Phys. Rev. B **75**, 235416-1–235416-7 (2007).
[23] B. Corzilius, K. P. Dinse, K. Hata, M. Haluška, V. Skákalová, and S. Roth, Phys. Status Solidi B **245**, 2251–2254 (2008).
[24] B. Nebendahl, D. N. Peligrad, M. Pozek, A. Dulcic, and M. Mehring, Rev. Sci. Instrum. **72**, 1876 (2001).
[25] R. Pound, Proc. IRE **35**(12), 1405–1415 (1947).
[26] F. Simon, H. Kuzmany, H. Rauf, T. Pichler, J. Bernardi, H. Peterlik, L. Korecz, F. Fülöp, and A. Jánossy, Chem. Phys. Lett. **383**, 362–367 (2004).
[27] F. Simon, C. Kramberger, R. Pfeiffer, H. Kuzmany, V. Zólyomi, J. Kürti, P. M. Singer, and H. Alloul, Phys. Rev. Lett. **95**, 017401-1–017401-4 (2005).
[28] F. Simon, H. Kuzmany, B. Náfrádi, T. Fehér, L. Forró, F. Fülöp, A. Jánossy, L. Korecz, A. Rockenbauer, F. Hauke, and A. Hirsch, Phys. Rev. Lett. **97**, 136801-1–136801-4 (2006).
[29] K. Hata, D. N. Futaba, K. Mizuno, T. Namai, M. Yumura, and S. Iijima, Science **306**, 1362–1365 (2004).
[30] P. T. Araujo, S. K. Doorn, S. Kilina, S. Tretiak, E. Einarsson, S. Maruyama, H. Chacham, M. A. Pimenta, and A. Jorio, Phys. Rev. Lett. **98**, 067401 (2007).
[31] K. P. Bohnen, R. Heid, H. J. Liu, and C. T. Chan, Phys. Rev. Lett. **93**, 245501-1–245501-4 (2004).
[32] D. Connétable, G. M. Rignanese, J. C. Charlier, and X. Blase, Phys. Rev. Lett. **94**, 015503-1–245501-4 (2005).

© 2012 WILEY-VCH Verlag GmbH & Co. KGaA, Weinheim